MJSAT

Malaysian Journal of Science and Advanced Technology

journal homepage: https://mjsat.com.my/

Preparation and Characterization of Oil Palm Empty Fruit Bunch-Based Cellulose for Levulinic Acid Production

Z.N. Akhlisah[1]*, W.A.K.G Wan Azlina[1], R. Yunus[1], Y.H. Taufiq-Yap[2], and U. Rashid[3]

[1] *Sustainable Process Engineering Research Centre (SPERC), Department of Chemical and Environmental Engineering, Faculty of Engineering, University Putra Malaysia, 43400 UPM Serdang, Selangor, Malaysia.*

[2] *Catalysis Science and Technology Research Centre, Faculty of Sciences, Universiti Putra Malaysia, 43400 UPM Serdang, Selangor, Malaysia*

[3] *Institute of Nanoscience and Nanotechnology, Universiti Putra Malaysia, Serdang 43400, Selangor, Malaysia.*

KEYWORDS

Cellulose
Oil palm empty fruit bunch
Characterization
Sugars
Levulinic acid

ARTICLE HISTORY

Received 15 July 2024
Received in revised form 29 July 2024
Accepted 12 August 2024
Available online 2 September 2024

ABSTRACT

This study investigates the process of isolating and characterizing cellulose from Oil Palm Empty Fruit Bunch (OPEFB) fibers collected from Sime Darby Plantation, Selangor. The OPEFB fibers underwent a sequence of chemical processes including dewaxing, alkali pretreatment and bleaching, to isolate the cellulose. The resulting cellulose was analyzed for its composition, crystallinity and yield of hydrolysis products. Comparative analysis with recent studies indicates that the cellulose content of the isolated fibers falls within the reported range, with relatively lower lignin content suggesting a successful lignin removal during chemical treatments. The crystallinity index of the cellulose significantly increased after the post-treatment, reaching 76.43%, which is higher than some reported values. The hydrolysis of the isolated cellulose from OPEFB yielded levulinic acid (LA) levels comparable to commercial cellulose, with the OPEFB-based cellulose producing an LA yield of 8.98% lower than the 9.73% from commercial cellulose. This study highlights the potential of OPEFB as a viable source of high-quality cellulose for the production of sugars and LA.

1. INTRODUCTION

The persistent challenge of energy, exacerbated by the overutilization of conventional energy sources, remains a significant issue globally [1]. This problem highlights the lack of affordable and reliable access to modern energy services, which are essential for promoting social and economic progress at the individual, community, and national levels [2]. With increasing awareness of the detrimental impacts of fossil fuels, there is a compelling drive to explore and adopt alternative energy sources that meet our energy needs while mitigating environmental harm [3]. This shift has led to growing interest in renewable energy sources such as solar, biomass, hydro, nuclear thermal, tidal, and mechanical energy sources [4]. Unlike fossil fuels, renewable energy sources are inexhaustible and continuously available. The inherent stability makes them dependable, especially during periods of high demand or disruptions in fossil fuel power generation [2]. Among renewable options, biomass energy stands out as a viable alternative. It encompasses various sources such as food processing waste, solid wastes, energy crops, human sewage, and residues from timber, forests, and agricultural crops [5]. Lignocellulosic biomass, in particular, is well-suited for producing pharmaceuticals, biofuels as well as value-added chemicals in many industrial applications [6].

Renewable materials derived from oil palm-based sources offer a low-sulfur, carbon-neutral, and widely available alternative to fossil-derived precursors. The oil palm tree or *Elaeis guineensis* originally from Africa, was introduced to Southern Asia and South America between the sixteenth and nineteenth centuries [7]. In 2020, Malaysia and Indonesia collectively accounted for 84% (63.9 million tons) of global output, with Malaysia contributing 25% and Indonesia

*Corresponding author:
E-mail address: Z.N. Akhlisah <akhlisahzn@gmail.com>.
https://doi.org/10.56532/mjsat.v4i3.348

contributing 59% [8]. Oil palm biomass waste includes various lignocellulosic residues generated during palm oil processing and cultivation, including palm oil mill effluent (POME) (60%), oil palm empty fruit bunches (OPEFB) (23%), mesocarp fiber (MF) (21%), palm kernel shell (PKS) (5%), oil palm fronds (OPF) and oil palm trunks (OPT) [9]. Notably, producing one tons of crude palm oil typically requires about five tons of oil palm fresh fruit bunches, significantly increasing waste generation [10]. The OPEFB, with its relatively low lignin concentrations ranging from 14.2% to 38.4%, is the most utilized biomass due to its ease of pre-treatment [11]. Annual OPEFB production totals approximately 17.64 million tons when wet or 5.29 million tons in dry form [12]. Thus, in order to maximize profitability and environmental sustainability, efficient utilization of OPEFB is crucial, extracting valuable chemical feedstock such as cellulose, hemicellulose, and lignin for various practical applications. The substantial cellulose content in OPEFB renders it a promising non-edible biomass source for producing valuable chemicals [13].

Cellulose, the most abundant polymer on Earth, offers a cost-effective option with robust mechanical properties and is extractable from various plants and biomass sources, including agro-waste (corncob, soybean pods, rice straw, etc.) and industrial agro-waste (oil palm waste, tomato peel, bagasse, etc.) [14]. Cellulose is a polymer composed of high molecular weight β−1,4-linked anhydro-D-glucose units in which a dimer of glucose residue is the repeating unit of cellulose [15]. Cellulose can be converted into hexose sugars such as glucose and fructose. According to Huber *et al. (*2006) [16], during the initial phase of cellulose hydrolysis, it is necessary to break the glucoside bonds between α-D-glucose units. The cleavage mechanism of the C-O-C bond in cellulose involves the protonation of glucoside bonds. The proton has the option to either target the cyclic oxygen or the oxygen bond connecting two glucose molecules. In acidic conditions, glucose converts to hydroxylmethylfurfural (HMF) and subsequently forms levulinic acid (LA) upon rehydration [17]. Hexose sugars are converted to LA by hydrolyzing HMF in equal amounts during HMF hydrolysis [18]. Levulinic acid (LA) is primarily synthesized through acid-catalyzed chemical processes, unlike other high-value biomass derivatives which are derived through biological pathways such as fermentation [19]. The C6-derived cellulose sugar glucose can undergo a series of acid-catalyzed reactions to yield LA, formic acid, and acetic acid [20].

Biomass-derived cellulose is utilized in diverse applications such as water filtration membranes, chemical precursors, electronic components, tissue engineering, packaging, textiles, drug delivery systems, and cosmetics [21]. Various techniques exist for extracting cellulose from lignocellulose biomass. The most economical methods for cellulose isolation involve the utilization of chemical, physical, or biological pretreatments to remove lignin, hemicellulose, and other non-cellulosic components [14]. Removing hemicellulose and lignin enlarged pores and enhanced substrate accessibility to catalysts or enzymes, thereby facilitating an improved biomass conversion process [22]. Efficient isolation procedures are crucial for effectively converting OPEFB into glucose yield via a hydrolysis reaction. Research by Ratnakumar *et al.,* (2022) [23] revealed the significant impact of initial biomass particle sizes on cellulose extraction efficiency. They observed that while cellulose content was high in the powdered biomass with particle size between 150 and 250 µm sample, a greater quantity of isolated cellulose was recorded in the sample with particle size less than 75 µm. This demonstrates that reducing the size of biomass can substantially increase isolated cellulose yield.

In this study, the fibers underwent a multistep pretreatment aimed at increasing the cellulose fraction and removing non-cellulosic components. Various cellulose extraction methods, including mechanical treatment to reduce fiber size, dewaxing, alkaline treatment as well as bleaching were investigated. To the best of our knowledge, there was no prior research that investigated the viability of cellulose extracted from OPEFB to produce sugars and LA. Most of the studies have used commercial cellulose as raw material [24–26]. Some previous studies used OPEFB directly, without first isolating the cellulose [27–29]. Hence, this study provides novel insights into the potential of OPEFB-derived cellulose for producing glucose, HMF, LA, and formic acid (FA). A thorough investigation was conducted using Thermal Gravimetric Analysis (TGA), X-ray Diffraction (XRD) and Fourier Transform Infrared Spectroscopy (FTIR) to reveal significant changes such as the disappearance of functional groups and changes in crystallinity in the material characteristics, indicating a successful extraction of cellulose from OPEFB.

2. MATERIALS AND METHODS

2.1. Materials

The primary material used for isolating cellulose was OPEFB collected directly from the conveyor post-shredding at Sime Darby Plantation, Felda Pulau Carey, Selangor. Other essential materials including commercial cellulose, sulfuric acid (H_2SO_4), sodium hydroxide (NaOH), ethanol, toluene, sodium chlorite ($NaClO_2$) and hydroxhloric acid (HCl) were procured from R&M Chemicals, UK and are of analytical grade. High Performance Liquid Chromatography (HPLC) standards such as glucose, HMF, LA and FA were purchased from Sigma Aldrich, Germany.

2.2. Raw Materials Preparation

In this study, OPEFB fiber was chosen as the primary material. After collection from the plantation, the fiber was subjected to a washing process with tap water to eliminate surface oil and debris. The shredded OPEFB fiber was then partially sun-dried before being completely dried in an oven (Model Memmert 600, Germany) at 105°C for 24 hours or until the moisture level dropped below 10%. After reaching room temperature, the fiber was ground using the Universal Cutting Mill (Fritsch GmbH, Germany). The resulting fiber was then sieved to an approximate length of 125 to 250 µm and stored in a tightly sealed plastic bag, following a method by Ratnakumar *et al.* (2022) [23].

2.3. Cellulose isolation

The cellulose isolation process involved a sequence of steps starting with dewaxing, followed by delignification using alkali pretreatment and a bleaching process. The dewaxing procedure was carried out as follows: 50 g of selected fiber was placed inside a cellulose thimble and then subjected to the Soxhlet extraction technique followed by the Technical Association of the Pulp and Paper Industry (TAPPI)

204 cm-97 test methods [30]. Fig. 1 depicts the specific apparatus configuration used for Soxhlet extraction for the dewaxing process. In this procedure, ground and sieved OPEFB fiber was submerged in a solvent blend consisting of ethanol and toluene in 1:2 ratios. The extraction was carried out for a minimum duration of 6 h, or until the solvent achieved clarity, resulting in dewaxed OPEFB lignocellulose fibers. The Soxhlet extraction process was conducted for a duration of 10 to 12 h, ensuring adequate time for the solvent in the Soxhlet tube to achieve the required clarity.

The large-scale production of cellulose for the next steps was accomplished through the implementation of a batch reaction which includes an oil-based heating mantle, a stirrer with adjustable rotation, and a condenser. The jacketed glass reactor with a maximum capacity of 5.0 L was used to carry out all pretreatment steps including alkali pretreatment, bleaching, and refluxing processes. The entire procedure consisted of three main steps. Firstly, an alkali pretreatment was carried out using a 5% wt NaOH solution at a temperature of 80 °C for a duration of 1 h. Subsequently, a bleaching pretreatment was performed by utilizing a 5% wt $NaClO_2$ solution at 90 °C for 2 h and repeated twice to ensure the effectiveness. Lastly, the process concluded with a refluxing step using a 2% HCl solution for 2 h. Filtration was employed to separate the insoluble fiber residue which was subsequently washed with tap water and finally rinsed with distilled water until it became neutral. As a final step, the fiber was oven-dried overnight to eliminate moisture and subsequently ground using a grinder to produce cellulose powder [31,32].

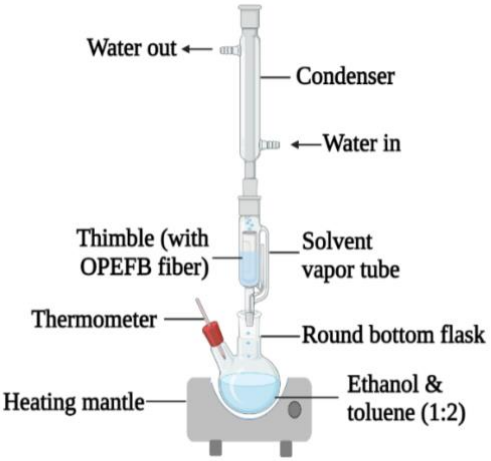

Fig. 1. Soxhlet extraction for the dewaxing process

2.4. Characterization studies

The Van Soest's acid detergent fiber (ADF), neutral detergent fiber (NDF), and acid detergent lignin (ADL) analysis methods were employed to determine the amount of lignin, cellulose, hemicellulose, and ash in OPEFB [33]. For compositional analysis, the prepared OPEFB was sent to the Malaysian Agriculture Research and Development Institute (MARDI), Serdang. The percentages of cellulose, hemicellulose, lignin, and extractives were calculated using the Goering and Van Soestt (1970) equation as shown below:

$$Cellulose\ (\%) = ADF - ADL \quad (1)$$

$$Hemicellulose\ (\%) = NDF - ADF \quad (2)$$

$$Lignin\ (\%) = ADL \quad (3)$$

$$Extractives\ (\%) = 100 - NDF\ (\%) \quad (4)$$

The FTIR spectra were recorded using the Thermo Fisher Scientific, Nicolet 6700 infrared spectrophotometer in a scanning range of 550–4000 cm^{-1}. Thermal gravimetric analysis (TGA) measurements were conducted on a thermal analyzer Mettler Toledo Model: TGA-DSC HT-3 for both TGA and differential thermal analysis (DTG). X-ray Diffraction (XRD) analysis was performed by Shimadzu, XRD 6000 diffractometer utilizing Cu-Ka radiation electrons generated by a Philips diffraction X-ray tube with a wavelength λ, = 0.1541 nm, a voltage of 30 kV and a generator current of 30 mA. The calculation of the the degree of crystallinity or crystalline index (CrI) of the samples can be done using the equation (5):

$$CrI = \frac{Area\ all\ crystalline\ peaks}{Area\ crystalline\ peaks + Amorphous\ peaks} \quad (5)$$

where CrI denotes the crystalline index or degree of crystallinity of material (unitless).

2.5. Conversion into levulinic acid (LA)

The cellulose obtained was assessed for its ability to produce LA. 1 gram of cellulose was utilized in the hydrolysis reaction at 160 ºC for 2 h using sulfonated carbon metal catalyst synthesized through the following method: cellulose was carbonized at 400 ºC for 1 h and subsequently sulfonated using H_2SO_4 solution for 12 h at 150 ºC. Following that, the carbon material was impregnated with metals. The resulting LA yield was then compared with LA generated from commercial cellulose. After the reaction, the solid phase was separated from the aqueous phase. Concentrations of glucose, HMF, FA, and LA were quantified using an HPLC system equipped with RI-detection (Infinity 1260, Agilent, Santa Clara, USA) and a Phenomenex Rezex-RFQ column (100 x 7.8 mm, 8 µm particle size). The mobile phase for analysis consisted of 0.01 M H_2SO_4 in water [34,35]

3. RESULT AND DISCUSSIONS

3.1. OPEFB Characterization

Fig. 2 shows a prepared OPEFB sample that was washed and screened to remove unwanted materials, ground, and sieved to an approximate length of 125 to 250 µm.

Fig. 2. OPEFB sample after dried, ground and sieved

The proximate analysis in Table 1 indicates the findings of analysis by neutral detergent fiber (NDF), acid detergent

fiber (ADF), acid detergent lignin (ADL), and ash. These data are shown as percentages, representing the composition per 100 grams of OPEFB or on a dry basis.

Table 1. Proximate analysis of OPEFB

Analysis	Content (%)
Acid Detergent Fiber (ADF)	56.76
Neutral Detergent Fiber (NDF)	77.43
Acid Detergent Lignin (ADL)	14.82

Table 2 shows the amount of cellulose, hemicellulose, lignin, ash, and extractives expressed as percentages based on a quantity of 100 g of OPEFB (or on a dry basis) in comparison with recent studies. The cellulose content in OPEFB fibers in this research compares with the range reported in the literature, with values ranging from 39.90% to 48.60%. The hemicellulose content was also consistent with values recorded by previous studies which varied from 13.30% to 29.80%. Nevertheless, it is important to mention that the amount of lignin in our study (14.82%) is generally lower in comparison to some previous studies, where the lignin content may have reached as high as 25.20% from a study by Zarin *et al.* (2022) [25]. The amount of extractives is high in this study compared to other reports, hence, the dewaxing method is needed to remove the extractives for subsequent usage of OPEFB [37].

Variations in chemical composition observed among different studies can be attributed to several reasons, including harvesting technique, growth conditions, and biomass storage practices [38]. Additionally, differences in processing techniques and analytical procedures during biomass composition can influence the reported results [39]. Given that lignocellulosic materials constitute a substantial amount of biomass, it is crucial to assess the chemical composition before conducting any experiments. Understanding the chemical composition of OPEFB fiber is important for further isolation of cellulose to remove hemicellulose, lignin, and extractives.

Table 2. Compositional analysis of OPEFB

Research	Materials (%)			
	Cellulose	Hemicellulose	Lignin	Extractive
This study*	41.94	20.67	14.82	22.57
[29]	40.30	19.90	22.90	16.90
[53]	42.38	23.84	20.20	-
[25]	41.00	13.30	25.20	20.50
[30]	39.90	25.80	22.10	12.20
[15]	44.60	29.80	21.40	4.13
[31]	48.60	28.10	23.40	-

*The proximate analysis data from MARDI for this study was issued by the Agriculture Chemical Analysis Laboratory (D10), Food and Agriculture Analysis Laboratory Program, Technical Services Center.

'-' Not determined.

The thermogravimetric curves of lignocellulosic biomass exhibit four different stages of primary decompositions, characterized by the reduction in weight of the biomass materials (hemicellulose, cellulose, and lignin) and the loss of moisture. After the removal of moisture up to a temperature of 150 ºC, the decomposition of the three biomass lignocellulosic components is observed. Hemicellulose undergoes degradation at temperatures ranging from 230 to 290 ºC, while cellulose degrades at temperatures between 290 and 370 ºC [43]. However, the decomposition peak of lignin was broader in comparison to the decomposition peaks of hemicellulose and cellulose due to the lower reactivity of C-C bonds in lignin [44]. In the last stage, the slow and constant decomposition of the complex compound lignin occurred at a temperature of 370 to 900 °C [45]. According to the TGA result shown in Fig. 3, the cellulose content is approximately 38.98% (stage III), the hemicellulose content is 21.41% (stage II), and the lignin content is 10.45% (stage IV). The values for cellulose, hemicellulose, and lignin in the proximate analysis were 41.94%, 20.67%, and 14.82%, respectively, which are not markedly different from these results. The content of residue collected from TGA analysis is 23.41% which is almost equal to the result from proximate analysis.

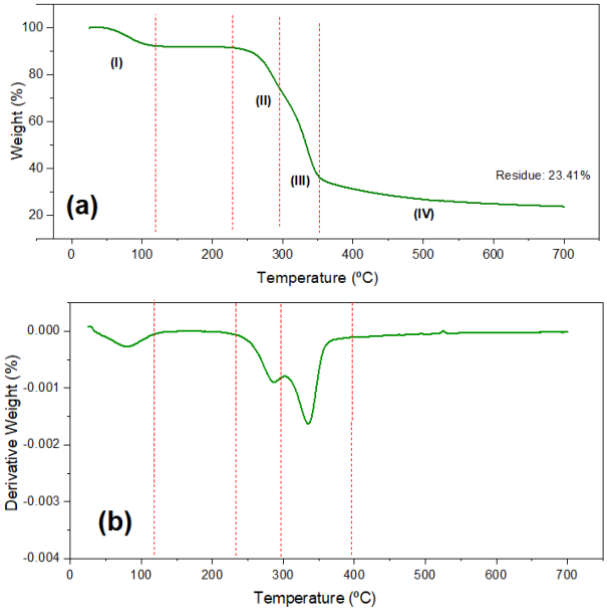

Fig. 3. TG (a) and DTG (b) Curve for prepared OPEFB

3.2 Characterization of cellulose isolated from OPEFB

Fig. 4 shows the physical transformation from a raw OPEFB fiber to cellulose obtained through an isolation process involving a dewaxing technique, treatment using NaOH, bleaching treatment using $NaClO_2$ solution, and refluxing using HCl solution. The change in color primarily results from the removal of lignin, a complex aromatic polymer that imparts a brown color to natural fibers. NaOH treatment disrupts the lignin structure, while $NaClO_2$ treatment further breaks down lignin into soluble fragments that are washed away, leaving behind the white cellulose. Consequently, the original brown color of raw OPEFB fiber turns white post-isolation due to the removal of hemicellulose and lignin materials [46]. A study carried out by Ng *et al.*, (2015) [36] corroborated that successful cellulose isolation is typically indicated by a noticeable color change to a white powder. Similar observations have been reported in cellulose isolation from other biomass sources such as sugarcane bagasse [32] and rice husks [48], where the color alteration serves as an indicator of effective removal of lignin and hemicellulose.

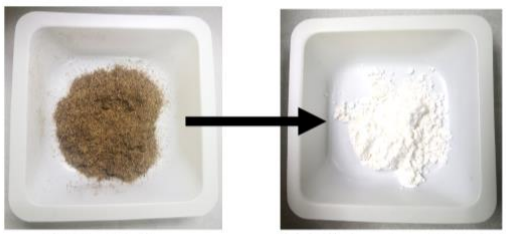

Fig. 4. OPEFB fiber and cellulose produced from OPEFB

Meanwhile, the evaluation based on chemical properties was observed from the analysis of TGA, XRD, and FTIR below.

The purpose of TGA analysis is to differentiate the decomposition behaviors of hemicellulose and cellulose materials in both the original OPEFB sample and isolated cellulose from OPEFB (OPEFB-based cellulose). Hemicellulose undergoes degradation at temperatures ranging from 230 to 290 ºC, while cellulose degrades at temperatures between 290 and 370 ºC [43]. Lignin, on the other hand, degrades at a temperature above 400 ºC [49]. The distinct decomposition profiles of these materials are evident in the TGA and DTG curves depicted in Fig. 5. The TGA results for the OPEFB-based cellulose sample exhibit distinct decomposition trends compared to those of the original OPEFB sample.

Both samples exhibit a degradation peak corresponding to the thermal breakdown of cellulose within a narrow temperature range of 290 to 370 °C consistent with findings from previous studies. However, the decomposition peak within the temperature range of 230 to 290 ºC, indicative of hemicellulose degradation, appears only in the OPEFB sample, suggesting the absence of hemicellulose in the isolated cellulose (OPEFB-based cellulose) sample. The disappearance of this peak confirms that the alkaline and bleaching treatment has effectively removed the unstable hemicellulose [50]. The findings align with the TGA result for isolated cellulose obtained in the study by Ajayi *et al.* (2023) [15] and Mirzaee *et al.* (2023) [41], where only cellulose degradation was observed in isolated cellulose samples. The hydrolysis of glycosidic bonds in cellulose, resulting in the production of water, alkenes, carbon dioxide, and other hydrocarbon derivatives which performed within the temperature range of 250–370 ºC. The degradation and DTG peak temperature of isolated cellulose were lower than OPEFB biomass. This difference may be attributed to the significant reduction in the molecular weight of OPEFB biomass resulted from acid hydrolysis during refluxing steps [52].

Furthermore, the residual weight remaining after thermal degradation in TGA is higher in the raw OPEFB sample compared to the isolated cellulose. This higher residual weight indicates that the raw OPEFB contains more inorganic material, such as ash, which does not decompose during TGA analysis [52]. The isolation process in this study has effectively reduced these inorganic constituents, resulting in a lower residual weight for the isolated cellulose sample and highlighting the achievement of the purification step. In addition, the isolated cellulose in this study showed good thermal stability compared to commercial cellulose. It was expected that the yield of hydrolysis products from isolated cellulose would be lower than commercial cellulose since the conversion of high thermal stability cellulose requires extensive hydrolysis conditions [52].

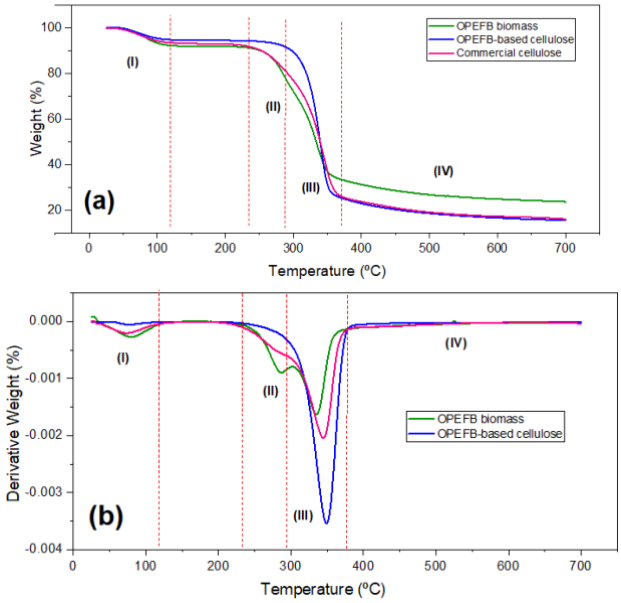

Fig. 5. Comparison of TGA curve (a) and DTG curve (b) for OPEFB biomass and OPEFB-based cellulose

FTIR spectra for OPEFB-based cellulose are presented in Fig. 6 with a raw OPEFB sample provided alongside for comparative purposes. Peaks around 3200-3400 cm^{-1} in both samples were assigned to the O–H stretching vibration of the hydrogen-bonded hydroxyl group in the cellulose molecule [53]. Furthermore, C–H stretching groups of cellulose were seen at 2885 cm^{-1} in both samples. The presence of significant micro-cellulose content is confirmed by the C–OH vibration in both samples, which exhibits a very intense band at 1032 cm^{-1} [54]. In the raw OPEFB, a peak at 1373 cm^{-1} is attributed to the bending vibrations of C-O of cellulose [55]. Interestingly, this peak appears more pronounced in the sample of OPEFB-based cellulose.

In the FTIR spectra, the C=O stretching frequency of the carbonyl functional groups from hemicellulose and lignin fractions was observed in the OPEFB sample at 1720 cm^{-1}. Another distinctive peak present only in the spectrum of OPEFB is at 1238 cm^{-1}, attributed to the syringyl ring and C–O stretching of lignin and xylan [50]. The complete absence of these peaks in the spectrum of the OPEFB-based cellulose sample indicates that the isolation process effectively removed or significantly reduced the presence of hemicellulose and lignin. Furthermore, the intensity of the peak located at 1613 cm^{-1} which is related to the C=C stretching of aromatic rings in lignin, was noticeably diminished in the OPEFB-based cellulose sample. These findings are consistent with Kaur *et al.,* (2023) [46] and Kundu *et al.,* (2023) [14] where isolated cellulose from biomass similarly resulted in the disappearance or reduction of these special features.

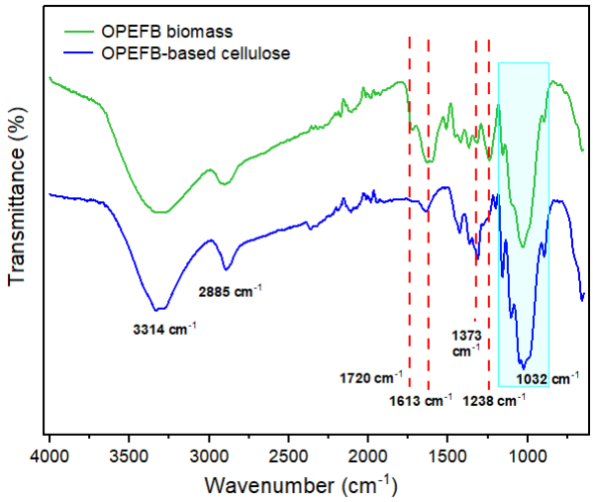

Fig. 6. Comparison of FTIR analysis for OPEFB biomass and OPEFB-based cellulose

Fig. 7 shows the XRD patterns of OPEFB-based cellulose and similar to FTIR analysis, a raw OPEFB sample is provided alongside for comparative purposes. This analysis was conducted to evaluate the phase purity and crystallinity of the OPEFB before and after the cellulose isolation process. The XRD pattern of the OPEFB sample was broad and did not show any sharp peaks. Only one peak appeared in this sample. This reveals that the sample had an amorphous structure which is similar to findings by Mirzaee *et al.*, (2023) [41]. The XRD pattern of the OPEFB-based cellulose shows a prominent peak at $2\theta = 22.5^{o}$, characteristic of cellulose I, indicating a highly crystalline structure. This peak is significantly more pronounced compared to the XRD pattern of the raw OPEFB, which exhibited a broad and diffuse peak, signifying its amorphous nature. The elimination of lignin and hemicellulose which was verified by the FTIR findings, both known to be amorphous in the raw material, results in a sharper and more distinct appearance of the crystalline peak, reflecting the improved crystallinity. This transition from an amorphous to crystalline structure underscores the effectiveness of the cellulose isolation process.

The CrI increased to 76.43% compared to raw OPEFB (18.58%) and was higher than that reported in the literature for cellulose isolated from other agricultural sources. For example, Ndwandwa *et al.*, (2023) [47] obtained 63.82% and 72.10% crystallinity of cellulose derived from bagasse and eucalyptus, respectively. Mirzaee *et al.* (2023) [41] reported a CrI of 70.0% for cellulose extracted from rapeseed straw while 64.48% crystallinity of cellulose from OPEFB was reported by Norazli *et al.* (2023) [42]. The higher CrI observed in our study indicates a more efficient removal of amorphous components, particularly hemicellulose and lignin, resulting in a cellulose product with improved structural order.

The process of isolating cellulose from OPEFB involves several critical methods, including dewaxing, alkali pretreatment (delignification), and bleaching, each contributing to the removal of non-cellulosic components and enhancing the cellulose crystallinity. Alkali pretreatment, also known as delignification, specifically targets the lignin and partially removes hemicellulose, effectively breaking down the amorphous regions.

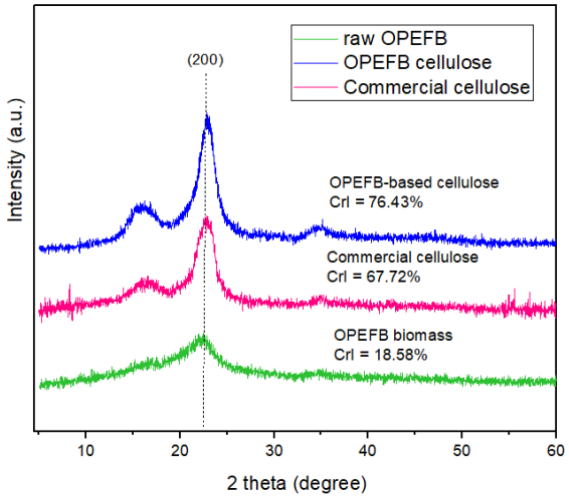

Fig. 7. XRD analysis for OPEFB biomass, OPEFB-based cellulose and commercial cellulose

This is evidenced by the disappearance of the broad, amorphous peak in the XRD pattern of the raw OPEFB sample. The subsequently bleaching process further purifies the cellulose, resulting in clearer and more distinct crystalline peaks in the XRD pattern. This process ensures the removal of residual lignin and other impurities, enhancing the overall quality of the isolated cellulose. The combined effect of these methods not only increased the CrI but also removed amorphous regions, thereby improving the overall quality and crystallinity of the isolated cellulose.

3.3 Evaluation of cellulose conversion in the hydrolysis reaction

The evaluation of the cellulose obtained from the extraction process was done by subjecting this material to a hydrolysis reaction. The yields of various products including glucose, HMF, FA, and LA generated from this hydrolysis reaction of extracted cellulose were compared with products collected from the reaction using commercial cellulose. Table 3 presents the yield of glucose, HMF, FA and LA from OPEFB-based cellulose and commercial cellulose. The yield of LA from OPEFB-based cellulose is 8.98% (based on theoretical yield), slightly lower than the 9.73% yield from commercial cellulose. However, this difference is within an acceptable range considering the physical and chemical properties of cellulose and other factors such as natural variability in cellulose sources, processing, and isolation techniques [15]. Furthermore, the difference between the two yields is small, indicating the level of purity of OPEFB-based cellulose.

Table 3. Product yields from different celluloses

Starting materials	**Yield (%) based on theoretical yield**			
	Glucose	**HMF**	**FA**	**LA**
Commercial cellulose	15.3	0.57	7.34	9.73
OPEFB-based cellulose	14.7	1.93	5.13	8.98

It is important to highlight that the total yields of LA from both starting materials are low as shown in Table 3. The slight reduction in LA yield from OPEFB-based cellulose can be attributed to its higher crystallinity index, thermal stability, and the complexity of the cellulose structure which have been

proved based on TGA and XRD results. Fig. 5 demonstrated the thermal stability of commercial cellulose is lower compared to OPEFB-based cellulose. Meanwhile, Fig. 7 indicated the crystallinity of commercial cellulose is also lower than the crystallinity of cellulose extracted from OPEFB. Highly crystalline cellulosic materials pose more difficulties and challenges in the process of converting cellulose into simpler molecules thereby affecting the overall yield of the reaction. This is due to the difficulty of the hydrolyzing agent in penetrating the matrix and the increased energy required to weaken the glycosidic bond of cellulose [57].

Comparing LA yields in this study with those reported in the literature highlights the potential and constraints of the existing hydrolysis process. Gromov et al. (2018) [58] achieved a yield of only 4.6% of LA by using solid acid catalysts made from a graphite-like mesoporous carbon material called Sibunit similar to the sulfonated carbon catalyst used in this study. Their lower yield suggests that the hydrolysis method employed in this study is more efficient than some previous studies that also used solid acid catalysts despite its relatively low total yield. In contrast, Han et al. (2019) [59] achieved a significantly higher production yield of 48.45% LA by employing a solid catalyst derived from lignin which was also a sulfonated carbon catalyst. However, their study also utilized γ-valerolactone (GVL) as a solvent in the reaction to produce LA. GVL facilitates the adsorption of cellulose and the reactive sites of the solid acid, accelerating the hydrolysis of cellulose into glucose [60]. The notable yield of this experiment demonstrates the potential for substantial enhancement in LA synthesis through the investigation of different catalysts and solvents in the hydrolysis process. It is worth noting that the high yield of LA in their research is partly attributed to the use of GVL, which facilitates the challenging conversion of cellulose into glucose. However, GVL is an expensive solvent, limiting its practicality for large-scale industrial applications [61].

It is noteworthy to highlight the generation of glucose, which is an important intermediate in the hydrolysis of cellulose to LA. The current study showed that 15.3% glucose was generated from commercial cellulose and 14.7% from OPEFB-based cellulose. These yields are comparatively low, indicating that the hydrolysis of cellulose into glucose remains a bottleneck in the process. The findings from a study by Han et al. (2019) [59], where the presence of GVL has significantly increased the conversion efficiency, suggest that improving glucose production could enhance the overall yield of LA. The relatively low glucose yields in this study align with the challenges mentioned in the previous studies, emphasizing the requirement for optimizing hydrolysis conditions to facilitate better yield of glucose. This highlights the necessity for additional optimization and pretreatment of cellulose to improve the efficiency of the production of LA.

4. CONCLUSION

The cellulose isolation from OPEFB fibers was successfully accomplished through a series of chemical processes, resulting in a product of high crystallinity and purity. The study confirmed that the cellulose content in the isolated fibers aligned with previous research, while the lignin content was notably lower. The crystallinity index of the isolated cellulose was significantly higher compared to raw OPEFB and some existing literature, suggesting successful elimination of amorphous components such as lignin and hemicellulose. The hydrolysis experiments revealed that the yield of LA from OPEFB-based cellulose (8.98% based on theoretical yield) was comparable to that from commercial cellulose (9.73% based on theoretical yield), albeit slightly lower. This suggests that the extracted cellulose is of high quality, yet further optimization of pre-treatment and hydrolysis processes is essential to enhance LA synthesis efficiency. In conclusion, this study underscores the potential of OPEFB fiber as a sustainable source of cellulose, with significant implications for various industrial applications.

ACKNOWLEDGEMENT

The authors would like to express their deepest appreciation to the Biobased Research Group UPM, PutraCat UPM and MPTL UPM for their technical assistance and collaboration. They also acknowledge the generous funding provided by DAAD and SEARCA.

REFERENCES

[1] Z. Wei, Z. Cheng, Y. Shen, Recent development in production of pellet fuels from biomass and polyethylene (PE) wastes, Fuel 358 (2024) 130222. https://doi.org/10.1016/j.fuel.2023.130222.

[2] J. Zhang, Energy access challenge and the role of fossil fuels in meeting electricity demand: Promoting renewable energy capacity for sustainable development, Geosci. Front. 15 (2024) 101873. https://doi.org/10.1016/j.gsf.2024.101873.

[3] J. González-Arias, G. Torres-Sempere, F. Arroyo-Torralvo, T.R. Reina, J.A. Odriozola, Optimizing biogas methanation over nickel supported on ceria-alumina catalyst: Towards CO2-rich biomass utilization for a negative emissions society, Environ. Res. 242 (2024). https://doi.org/10.1016/j.envres.2023.117735.

[4] G. Ezhumalai, M. Arun, A. Manavalan, R. Rajkumar, K. Heese, A Holistic Approach to Circular Bioeconomy Through the Sustainable Utilization of Microalgal Biomass for Biofuel and Other Value-Added Products, Microb. Ecol. 87 (2024). https://doi.org/10.1007/s00248-024-02376-1.

[5] D. Gayen, R. Chatterjee, S. Roy, A review on environmental impacts of renewable energy for sustainable development, Int. J. Environ. Sci. Technol. 21 (2024) 5285–5310. https://doi.org/10.1007/s13762-023-05380-z.

[6] X. Fan, M. Ren, C. Zhou, F. Kong, C. Hua, O.A. Fakayode, C.E. Okonkwo, H. Li, J. Liang, X. Wang, Total utilization of lignocellulosic biomass with xylooligosaccharides production priority: A review, Biomass and Bioenergy 181 (2024) 107038. https://doi.org/10.1016/j.biombioe.2023.107038.

[7] N.Z.J. Zakaria, S. Rozali, N.M. Mubarak, S. Ibrahim, A review of the recent trend in the synthesis of carbon nanomaterials derived from oil palm by-product materials, Springer Berlin Heidelberg, 2024. https://doi.org/10.1007/s13399-022-02430-3.

[8] A.S.A. Hamed, M.S. Yahya, N.A.A. Latiff, N.I.F.M. Yusof, N.F. Munajat, Thermochemical conversion of oil palm biomass and its applications: A bibliometric exploration of global trends over two decades, J. Anal. Appl. Pyrolysis 181 (2024) 106568. https://doi.org/10.1016/j.jaap.2024.106568.

[9] P. Parthasarathy, M. Alherbawi, M. Shahbaz, H.R. Mackey, G. McKay, T. Al-Ansari, Conversion of oil palm waste into value-added products through pyrolysis: a sensitivity and techno-economic investigation, Biomass Convers. Biorefinery 14 (2024) 9667–9687. https://doi.org/10.1007/s13399-022-03144-2.

[10] E.S. Tugiman, M.Z. Mohd Yusoff, M.A. Hassan, M.Y. Abd Samad, M.A. Ahmad Farid, Y. Shirai, Assessing the efficacy of utilizing biochar derived from oil palm biomass as a planting medium for promoting the growth and development of oil palm seedlings, Biocatal. Agric.

Biotechnol. 58 (2024) 103203. https://doi.org/10.1016/j.bcab.2024.103203.

[11] A.S. Gill, K.H. Wong, S. Lim, Y.L. Pang, L. Ling, S.Y. Lau, Investigation of Microwave Irradiation and Ethanol Pre-Treatment toward Bioproducts Fractionation from Oil Palm Empty Fruit Bunch, Sustain. 16 (2024). https://doi.org/10.3390/su16031275.

[12] M. Mahardika, A. Zakiyah, S.M. Ulfa, R.A. Ilyas, M.Z. Hassan, D. Amelia, V.F. Knight, M.N.F. Norrrahim, Recent Developments in Oil Palm Empty Fruit Bunch (OPEFB) Fiber Composite, J. Nat. Fibers 21 (2024). https://doi.org/10.1080/15440478.2024.2309915.

[13] C.A. Curie, L.W. Muslim, E.R. Safitra, S. Setyahadi, M. Gozan, Preliminary membrane screening and evaluation for the separation of bioethanol obtained from fermentation of oil palm empty fruit bunch (OPEFB), South African J. Chem. Eng. 48 (2024) 337–345. https://doi.org/10.1016/j.sajce.2024.03.001.

[14] S. Kundu, D. Mitra, M. Das, Influence of chlorite treatment on the fine structure of alkali pretreated sugarcane bagasse, Biomass Convers. Biorefinery 13 (2023) 567–581. https://doi.org/10.1007/s13399-020-01120-2.

[15] S.M. Ajayi, S.O. Olusanya, K.O. Sodeinde, A.E. Didunyemi, M.O. Atunde, D.P. Fapojuwo, E.G. Olumayede, O.S. Lawal, Hydrophobic modification of cellulose from oil palm empty fruit bunch: Characterization and application in Pickering emulsions stabilization, Carbohydr. Polym. Technol. Appl. 5 (2023) 100282. https://doi.org/10.1016/j.carpta.2023.100282.

[16] G.W. Huber, S. Iborra, A. Corma, Synthesis of Transportation Fuels from Biomass : Chemistry, Catalysts and Engineering, Chem. Rev. 106 (2006) 4044–4098.

[17] M.S.A. Pradipta, N.R. Purnamasari, Y.S. Pradana, Levulinic acid synthesis from Indonesian sugarcane bagasse using two-step acid catalyzed treatment, AIP Conf. Proc. 2085 (2019) 1–8. https://doi.org/10.1063/1.5095043.

[18] D. Rackemann, W. Doherty, A review on the production of levulinic acid and furanics from sugars, Int. Sugar J. 115 (2013) 28–34.

[19] A. Kumar, D. Shende, K. Wasewar, Central Composite Design Approach for Optimization of Levulinic Acid Separation by Reactive Components, Ind. Eng. Chem. Res. 60 (2021) 13692–13700. https://doi.org/10.1021/acs.iecr.1c02589.

[20] Z.N. Akhlisah, R. Yunus, Z.Z. Abidin, B.Y. Lim, D. Kania, Pretreatment methods for an effective conversion of oil palm biomass into sugars and high-value chemicals, Biomass and Bioenergy 144 (2021) 105901. https://doi.org/10.1016/j.biombioe.2020.105901.

[21] E. Eddiyanto, M. Ilham, F.A. Daulay, A.F.R. Piliang, J.D. Siregar, S. Gea, The synthesis of macro-initiator using cellulose isolated from OPEFB via atomic transfer radical polymerization method, AIP Conf. Proc. 3026 (2024). https://doi.org/10.1063/5.0200712.

[22] N. Hassan, N.A.K. Khairil Anwar, A. Idris, Strategy to enhance the sugar production using recyclable inorganic salt for pre-treatment of oil palm empty fruit bunch (OPEFB), BioResources 15 (2020) 4912–4931. https://doi.org/10.15376/biores.15.3.4912-4931.

[23] A. Ratnakumar, A.M.P.B. Samarasekara, D.A.S. Amarasinghe, L. Karunanayake, The influence of particle size on the extraction of cellulose nanofibers using chemical-ultrasonic process, Mater. Today Proc. 64 (2022) 274–278. https://doi.org/10.1016/j.matpr.2022.04.518.

[24] A.S. Khan, Z. Man, M.A. Bustam, C.F. Kait, A. Nasrullah, Z. Ullah, A. Sarwono, P. Ahamd, N. Muhammad, Dicationic ionic liquids as sustainable approach for direct conversion of cellulose to levulinic acid, J. Clean. Prod. 170 (2018) 591–600. https://doi.org/10.1016/j.jclepro.2017.09.103.

[25] A. Lorente, A.J. Huertas-Alonso, M. Salgado-Ramos, D.J. González-Serrano, M.P. Sánchez-Verdú, B. Cabañas, M. Hadidi, A. Moreno, Microwave radiation-assisted synthesis of levulinic acid from microcrystalline cellulose: Application to a melon rind residue, Int. J. Biol. Macromol. 237 (2023). https://doi.org/10.1016/j.ijbiomac.2023.124149.

[26] F. Yu, J. Thomas, M. Smet, W. Dehaen, B.F. Sels, Molecular design of sulfonated hyperbranched poly(arylene oxindole)s for efficient cellulose conversion to levulinic acid, Green Chem. 18 (2016) 1694–1705. https://doi.org/10.1039/c5gc01971k.

[27] L. Chuaboon, C. Saengsen, O. Sookbampen, E. Yang, H. Shukor, Y. Chisti, W. Rongwong, Enhanced Production of Levulinic Acid from Oil Palm Empty Fruit Bunch, Waste and Biomass Valorization (2024). https://doi.org/10.1007/s12649-024-02500-9.

[28] M. Gozan, J.R.H. Panjaitan, D. Tristantini, R. Alamsyah, Y.J. Yoo, Evaluation of Separate and Simultaneous Kinetic Parameters for Levulinic Acid and Furfural Production from Pretreated Palm Oil Empty Fruit Bunches, Int. J. Chem. Eng. 2018 (2018). https://doi.org/10.1155/2018/1920180.

[29] Y.W. Tiong, C.L. Yap, S. Gan, W.S.P. Yap, One-pot conversion of oil palm empty fruit bunch and mesocarp fiber biomass to levulinic acid and upgrading to ethyl levulinate via indium trichloride-ionic liquids, J. Clean. Prod. 168 (2017) 1251–1261. https://doi.org/10.1016/j.jclepro.2017.09.050.

[30] T. 204 Cm-97, Technical Association of the Pulp and Paper Industry: Solvent extractives of wood and pulp (TAPPI Standard Test Method T204 cm-97), 2007. https://doi.org/10.5772/916.

[31] N. Ndwandwa, F. Ayaa, S.A. Iwarere, M.O. Daramola, J.B. Kirabira, Extraction and Characterization of Cellulose Nanofibers From Yellow Thatching Grass (Hyparrhenia filipendula) Straws via Acid Hydrolysis, Waste and Biomass Valorization 14 (2023) 2599–2608. https://doi.org/10.1007/s12649-022-02014-2.

[32] W.R. Kunusa, R. Abdullah, K. Bilondatu, W.Z. Tulie, Analysis of Cellulose Isolated from Sugar Bagasse: Optimization and Treatment Process Scheme, J. Phys. Conf. Ser. 1422 (2020). https://doi.org/10.1088/1742-6596/1422/1/012040.

[33] P.J. Van Soest, J.B. Robertson, B.A. Lewis, Methods for Dietary Fiber, Neutral Detergent Fiber, and Nonstarch Polysaccharides in Relation to Animal Nutrition, J. Dairy Sci. 74 (1991) 3583–3597. https://doi.org/10.3168/jds.S0022-0302(91)78551-2.

[34] S. Bauer, A.B. Ibáñez, Does size matter? Separations on guard columns for fast sample analysis applied to bioenergy research, BMC Biotechnol. 15 (2015) 1–13. https://doi.org/10.1186/s12896-015-0159-3.

[35] L. Ribeiro Vasconcelos De Sá, R. De Oliveira Moutta, E. Pinto Da Silva Bon, M. Christe Cammarota, V.S. Ferreira-Leitão, Fermentative biohydrogen production using hemicellulose fractions: Analytical validation for C5 and C6-sugars, acids and inhibitors by HPLC, Int. J. Hydrogen Energy 40 (2015) 13888–13900. https://doi.org/10.1016/j.ijhydene.2015.08.014.

[36] M.A.A. Zarin, M.M. Zainol, N.A.S. Ramli, N.A.S. Amin, Zeolite immobilized ionic liquid as an effective catalyst for conversion of biomass derivatives to levulinic acid, Mol. Catal. 528 (2022) 112506. https://doi.org/10.1016/j.mcat.2022.112506.

[37] L.D. Mthembu, R. Gupta, N. Deenadayalu, Advances in Biomass-Based Levulinic Acid Production, Waste and Biomass Valorization 14 (2023) 1–22. https://doi.org/10.1007/s12649-022-01948-x.

[38] V. Pasangulapati, K.D. Ramachandriya, A. Kumar, M.R. Wilkins, C.L. Jones, R.L. Huhnke, Effects of cellulose , hemicellulose and lignin on thermochemical conversion characteristics of the selected biomass, Bioresour. Technol. 114 (2012) 663–669. https://doi.org/10.1016/j.biortech.2012.03.036.

[39] R. Biswas, H. Uellendahl, B.K. Ahring, Wet explosion pretreatment of sugarcane bagasse for enhanced enzymatic hydrolysis, Biomass and Bioenergy 61 (2014) 104–113. https://doi.org/10.1016/j.biombioe.2013.11.027.

[40] R. Masran, E.K. Bahrin, M.F. Ibrahim, L. Phang, S. Abd-aziz, Biocatalysis and Agricultural Biotechnology Simultaneous pretreatment and saccharification of oil palm empty fruit bunch using laccase-cellulase cocktail, Biocatal. Agric. Biotechnol. 29 (2020) 101824. https://doi.org/10.1016/j.bcab.2020.101824.

[41] L. Risanto, D.T.N. Adi, T. Fajriutami, H. Teramura, W. Fatriasari, E. Hermiati, P. Kahar, A. Kondo, C. Ogino, Pretreatment with dilute maleic acid enhances the enzymatic digestibility of sugarcane bagasse and oil palm empty fruit bunch fiber, Bioresour. Technol. 369 (2023) 128382. https://doi.org/10.1016/j.biortech.2022.128382.

[42] B.M. Harahap, M.R. Maulid, A.I. Dewantoro, E. Mardawati, S. Huda, Moderate pretreatment strategies for improvement of reducing sugar production from oil palm empty fruit bunches, IOP Conf. Ser. Earth Environ. Sci. 443 (2020). https://doi.org/10.1088/1755-1315/443/1/012081.

[43] D. Díez, A. Urueña, R. Piñero, A. Barrio, T. Tamminen, Determination of Hemicellulose, Cellulose, and Lignin Content in Di ff erent Types of Biomasses by Thermogravimetric Analysis and Pseudocomponent Kinetic Model, Processes 8 (2020) 1–21.

[44] P. Halder, S. Kundu, S. Patel, R. Parthasarathy, B. Pramanik, J. Paz-Ferreiro, K. Shah, TGA-FTIR study on the slow pyrolysis of lignin and cellulose-rich fractions derived from imidazolium-based ionic liquid pre-treatment of sugarcane straw, Energy Convers. Manag. 200 (2019) 112067. https://doi.org/10.1016/j.enconman.2019.112067.

[45] M.S. Reza, S.N. Islam, S. Afroze, M.S.A. Bakar, J. Taweekun, A.K. Azad, Data on FTIR, TGA – DTG, DSC of invasive pennisetum purpureum grass, Data Br. 30 (2020). https://doi.org/10.1016/j.dib.2020.105536.

[46] N.H.A. Rahman, B.W. Chieng, N.A. Ibrahim, N.A. Rahman, Extraction and characterization of cellulose nanocrystals from tea leaf waste fibers, Polymers (Basel). 9 (2017) 1–11. https://doi.org/10.3390/polym9110588.

[47] H.M. Ng, L.T. Sin, T.T. Tee, S.T. Bee, D. Hui, C.Y. Low, A.R. Rahmat, Extraction of cellulose nanocrystals from plant sources for application as reinforcing agent in polymers, Compos. Part B Eng. 75 (2015) 176–200. https://doi.org/10.1016/j.compositesb.2015.01.008.

[48] K. Bhandari, S. Roy, M. Arup, Á.M.Á. Rice, Synthesis and Characterization of Microcrystalline Cellulose from Rice Husk, J. Inst. Eng. Ser. E (2020). https://doi.org/10.1007/s40034-020-00160-7.

[49] M.K. Mohamad Haafiz, S.J. Eichhorn, A. Hassan, M. Jawaid, Isolation and characterization of microcrystalline cellulose from oil palm biomass residue, Carbohydr. Polym. 93 (2013) 628–634. https://doi.org/10.1016/j.carbpol.2013.01.035.

[50] B.W. Chieng, S.H. Lee, N.A. Ibrahim, Y.Y. Then, Y.Y. Loo, Isolation and characterization of cellulose nanocrystals from oil palm mesocarp fiber, Polymers (Basel). 9 (2017) 1–11. https://doi.org/10.3390/polym9080355.

[51] N. Mirzaee, M. Nikzad, R. Battisti, A. Araghi, Isolation of cellulose nanofibers from rapeseed straw via chlorine-free purification method and its application as reinforcing agent in carboxymethyl cellulose-based films, Int. J. Biol. Macromol. 251 (2023) 126405. https://doi.org/10.1016/j.ijbiomac.2023.126405.

[52] N. Norazli, N.F.M. Rawi, O.F.A. Taiwo, M.H.M. Kassim, M. Jawaid, Delignification's Effect on Microcrystalline Cellulose Obtained from Oil Palm Empty Fruit Bunch Fibres, BioResources 18 (2023) 1901–1915. https://doi.org/10.15376/biores.18.1.1901-1915.

[53] J.K. Ogunjobi, A.I. Adewale, S.A. Adeyemi, Cellulose nanocrystals from Siam weed: Synthesis and physicochemical characterization, Heliyon 9 (2023) e13104. https://doi.org/10.1016/j.heliyon.2023.e13104.

[54] M. Alhaji Mohammed, W.J. Basirun, N.M.M. Abd Rahman, N. Salleh, The Effect of Particle Size of Almond Shell Powders, Temperature and Time on the Extraction of Cellulose, J. Nat. Fibers 19 (2022) 5577–5587. https://doi.org/10.1080/15440478.2021.1881689.

[55] M.S. Nazir, B.A. Wahjoedi, A.W. Yussof, M.A. Abdullah, Eco-friendly extraction and characterization of cellulose from oil palm empty fruit bunches, BioResources 8 (2013) 2161–2172. https://doi.org/10.15376/biores.8.2.2161-2172.

[56] P. Kaur, H.B. Bohidar, F.M. Pfeffer, R. Williams, R. Agrawal, A comparative assessment of biomass pretreatment methods for the sustainable industrial upscaling of rice straw into cellulose, Cellulose 30 (2023) 4247–4261. https://doi.org/10.1007/s10570-023-05161-4.

[57] Y.W. Chen, H.V. Lee, Recent progress in homogeneous Lewis acid catalysts for the transformation of hemicellulose and cellulose into valuable chemicals , fuels , and nanocellulose 2 C atalytic transformation of ligno- cellulosic biomass components, Rev. Chem. Engeering 36 (2018) 215–235.

[58] N. V. Gromov, T.B. Medvedeva, O.P. Taran, A. V. Bukhtiyarov, C. Aymonier, I.P. Prosvirin, V.N. Parmon, Hydrothermal Solubilization–Hydrolysis–Dehydration of Cellulose to Glucose and 5-Hydroxymethylfurfural Over Solid Acid Carbon Catalysts, Top. Catal. 61 (2018) 1912–1927. https://doi.org/10.1007/s11244-018-1049-4.

[59] Y. Han, L. Ye, X. Gu, P. Zhu, X. Lu, Lignin-based solid acid catalyst for the conversion of cellulose to levulinic acid using γ-valerolactone as solvent, Ind. Crops Prod. 127 (2019) 88–93. https://doi.org/10.1016/j.indcrop.2018.10.058.

[60] D.W. Rackemann, J.P. Bartley, W.O.S. Doherty, Methanesulfonic acid-catalyzed conversion of glucose and xylose mixtures to levulinic acid and furfural, Ind. Crops Prod. 52 (2014) 46–57. https://doi.org/10.1016/j.indcrop.2013.10.026.

[61] Y. Jiang, L. Yang, C.M. Bohn, G. Li, D. Han, N.S. Mosier, J.T. Miller, H.I. Kenttämaa, M.M. Abu-Omar, Speciation and kinetic study of iron promoted sugar conversion to 5-hydroxymethylfurfural (HMF) and levulinic acid (LA), Org. Chem. Front. 2 (2015) 1388–1396. https://doi.org/10.1039/C5QO00194C.